17th World Conference on Earthquake Engineering, 17WCEE
Sendai, Japan - September 13th to 18th 2020

A STUDY ON HYSTERESIS MODELING OF REINFORCED CONCRETE COLUMNS

Y.C. Ling [1] and S.J. Hwang [2]

[1] *Ph.D. Student, Department of Civil Engineering, National Taiwan University, D08521005@ntu.edu.tw*
[2] *Professor, Department of Civil Engineering, National Taiwan University, sjhwang@ntu.edu.tw*

Abstract

Due to the higher modes of structural response, the nonlinear time-domain dynamic analysis is considered appropriate to perform the seismic evaluation of the mid- to high-rise buildings. The analysis must accurately reflect structural members' non-linear behaviors such as yielding strength, failure mechanism and hysteretic behavior. Columns as the major structural members in the lateral load-resisting systems. Hence, the hysteretic behavior prediction of columns is extremely importance in seismic design. In addition, there are a large amount of the reinforced concrete buildings which were built before the 1999 Chi-chi Earthquake in Taiwan. These old reinforced concrete buildings had lower seismic demands by code and were not detailed with the ductile reinforcement. Therefore, to assist the technology development for engineers on collapse prevention for the medium-to-high rise buildings in Taiwan, the proposed study aims at the development of the hysteretic models of reinforced concrete columns in different failure mode.

In this study, a hysteretic model of columns and its model parameters' formulas had been proposed based on the Pivot Hysteretic Model. A database of column specimens subject to cyclic loading has been collected from literature for the model optimization. The model optimization method was executed base on energy dissipation. Simulated annealing algorithm was used to calibrate the response with experimental results and to identify model parameters. Simultaneously, the relationship between the structural characteristics and model parameters was resolved by regression analysis, hypothesis testing and simulated annealing algorithm. The analytical results based on proposed model formulas can accurately reflect hysteretic behavior of columns such as unloading behavior and pinching effect in different failure mode.

Keywords: reinforced concrete column, hysteretic behavior, Pivot model, pinching effect

1. Introduction

In view of the earthquake disasters in 2016 Meinong earthquake and 2018 Hualien earthquake, more than 100 people lost their lives due to the collapse of mid- to high-rise buildings. According to the earthquake reconnaissance, these kinds of old reinforced concrete buildings were built before the 1999 Chi-Chi Earthquake. Most of them had lower seismic demands by code and were not detailed with the ductile reinforcement. To avoid these kinds of severe damages, it is necessary to enhance the technology on collapse prevention for the medium-to-high rise buildings.

With the technology development of seismic evaluation for buildings in Taiwan, the past studies focused on the prediction of lateral load-displacement curve for non-ductile columns. Li and Hwang [1] proposed the trilinear curve to simulate the seismic behavior of short columns failed in shear with the height-to-depth ratio of less than 2. Moreover, Li et al. [2] suggested the load-displacement curve for the intermediate short column failed in shear with the height-to-depth ratio of between 2 and 4. Both of researches have been applied to Taiwan Earthquake Assessment for Structures by Pushover Analysis (TEASPA) [3], which is a modified capacity spectrum method developed in the NCREE handbook for low-rise buildings seismic evaluation. However, due to the higher modes of structural response, the nonlinear time history analysis is considered appropriate to perform the seismic evaluation of the mid- to high-rise buildings. The analysis must accurately reflect structural members' non-linear behaviors such as yielding strength, failure mechanism and hysteretic behavior. Columns as the major vertical members to resist lateral loading in the RC frame structures. the hysteretic behavior prediction of columns included non-ductile detail is extremely importance in seismic evaluation. Hence, to assist the technology development on collapse prevention for the medium-to-high rise buildings, the proposed study aims at the development of the hysteretic models of reinforced concrete columns in different failure mode.

Several hysteretic models suitable to simulate the nonlinear behavior of RC members have been developed by different researchers. These models are characterized by piecewise linear force-displacement behavior. Early and well-known hysteretic models, such as bilinear degrading stiffness model [4], Takeda degrading stiffness model [5] and Pivot hysteretic model [6], have already been incorporated in commercial programs, such as ETABS and SAP2000. Of these, pivot hysteretic model is particularly well to suit the hysteretic behavior of columns due to its capability to accurately capture unloading stiffness and pinching effect. Furthermore, pivot hysteretic model is the only one having additional parameters to control the degrading hysteretic loop in ETABS and SAP2000.

Pivot hysteretic model was originally proposed for nonlinear dynamic analysis of RC circular columns. The model was developed based on the experimental observations on several cyclic tests on RC circular columns. These observations show that the unloading back to zero force from any displacement level is generally guided toward a single point on the idealized stiffness line. Similarly, all force-displacement paths tend to cross the elastic loading line at approximately the same point. The first point was called "primary pivot point" and the second point was called "pinching pivot" (Fig. 1). Thus, the model basically introduces model two parameters, α and β, to define these two points to control the unloading and pinching behavior of columns (Fig. 2).

To extend the application of Pivot hysteretic model on RC rectangular columns, Sharma et al. [7] proposed the parameters' formulas base on curve fitting of the test data and using regression analysis. The equations defining α and β were obtained as:

$$\alpha = 0.170 \times \rho_{\ell}/\mathrm{ALR} + 0.415 \tag{1}$$

$$\beta = 0.485 \times (\mathrm{ALR})^{0.25} \times (\rho_t)^{0.2} + 0.115 \tag{2}$$

$$\mathrm{ALR} = \frac{N}{A_g f'_c} \tag{3}$$

where ρ_ℓ is longitudinal reinforcement ratio; ALR is axial load ratio; ρ_t is volumetric ratio of shear reinforcement; N is axial load; A_g is gross cross-sectional area of the column; f_c' is compressive strength of concrete.

However, Sharma et al. [7] equations ignore the effect in different failure modes. The hysteretic behavior of column is extremely different in various failure mode. Columns in flexure failure mode have ductile nonlinear behavior. It means columns in flexure failure mode has larger deformation capacity, less stiffness degradation and less pinching effect. On the other hand, Columns failed in shear have brittle hysteretic behavior. Thus, it's necessary to reanalysis the parameters' equations for columns subject to different failure mode.

In this study, a hysteretic model of columns and its model parameters' formulas had been proposed based on the Pivot hysteretic model. To capture the hysteretic behavior of columns more accurately, the parameters' formulas are developed for columns subject to flexure failure and shear failure. A database of 80 column specimens subjected to cyclic loading has been collected from literature for the model optimization. The model optimization method by the proposed approach was executed base on energy dissipation. Simulated annealing algorithm was used to calibrate the response with experimental results and to identify model parameters. Simultaneously, the relationship between the structural characteristics and model parameters was resolved by regression analysis, hypothesis testing. Furthermore, parameters' formulas were also optimized base on energy dissipation. The analytical results based on proposed model formulas can accurately reflect hysteretic behavior of columns such as unloading behavior and pinching effect in flexure failure and shear failure mode.

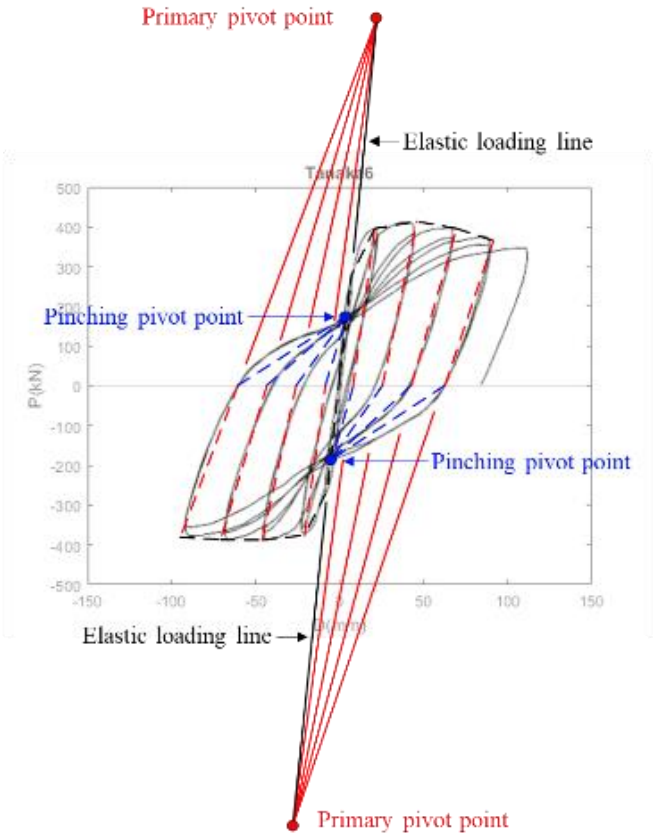

Fig. 1. Typical load-displacement behavior of RC column.

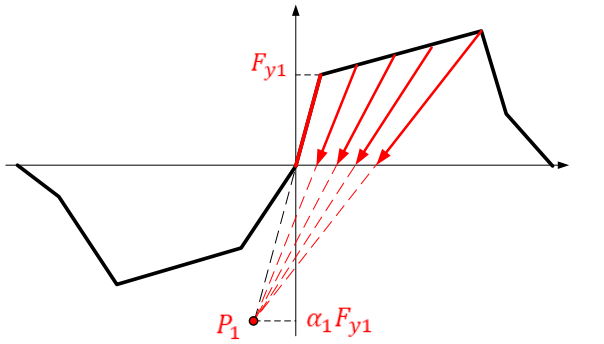

(a) Primary pivot point (parameter α controls)

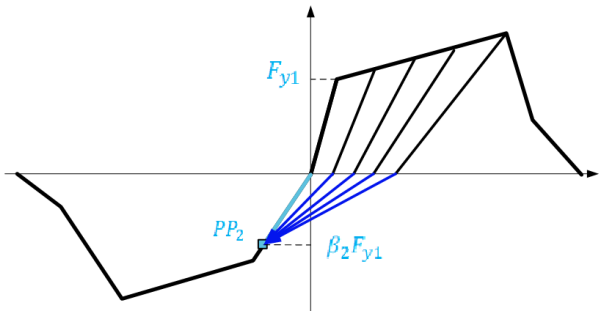

(b) Phinching pivot point (parameter β controls)

Fig. 2. Defination of pivot point

2. Column database used in this study

In this study, A database of 77 column specimens subject to cyclic loading has been collected from literature to calibrate the analytic model with the experimental results. To make sure the experimental hysteretic loops are enough to include all the hysteretic behavior within the allowable nonlinear range, which is defined from crack to 0.8 P_{max} after reaching the maximum load (Fig. 3), and to keep the modeling quality, there are five selection rules need to be obeyed.

Rule 1: Axial load ratio must be less than 0.6 to make the experimental condition same as building column.

Rule 2: The load history is Monolithically Increasing.

Rule 3: More than 3 cycles with different drifts (Fig. 4).

Rule 4: Each hysteretic loop cannot contain 2 physical characteristics, for instance, crack point and strenth point (Fig. 5).

Rule 5: Hysteretic loop should be nearly symmetric (Fig. 6)

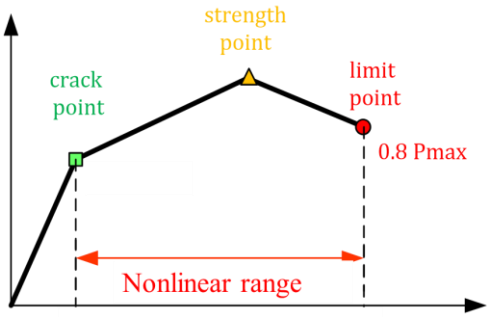

Fig. 3. Allowable nonlinear range

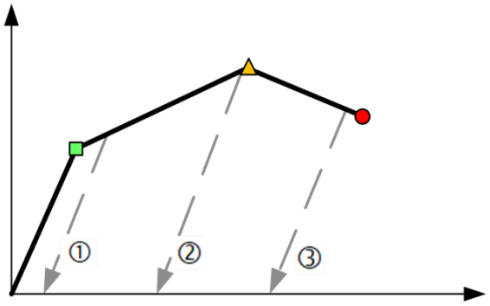

Fig. 4. Selection Rule 3.

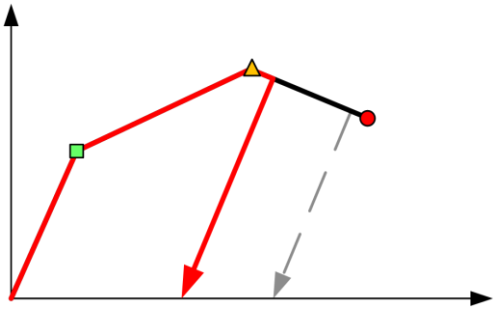

Fig. 5. Selection Rule 4.

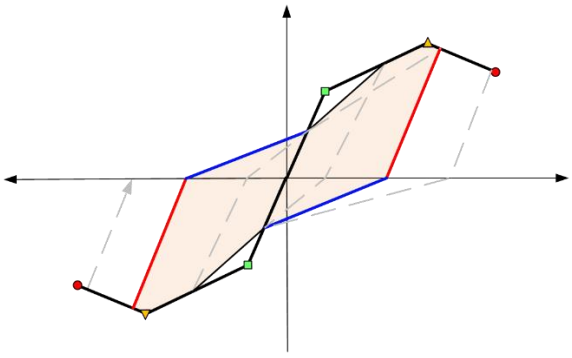

Fig. 6. Selection Rule 5.

For failure mode classification, V_{mn}/V_n is used as the parameter to classify the column datasets into flexure failure and shear failure group. V_{mn} is the shear strength at the nominal moment capacity, which is calculated by Xtract. V_n is the nominal shear strength. If V_{mn}/V_n greater than 1, the colomn dataset belongs to shear failure group, otherwise, if V_{mn}/V_n less than 1, the column dataset belongs to flexure failure group, including flexure and flexure-shear failure. The summary of the specimens has been enlisted in Table 1. There are 45 column specimens in flexure failure group and 30 column specimens in shear failure group.

Table 1. the summary of the column specimens

Flexure failure group ($V_{mn}/V_n < 1$)									
Researchers	Specimen	ALR	ρ_ℓ (%)	ρ_t (%)	Researchers	Specimen	ALR	ρ_ℓ (%)	ρ_t (%)
Gill *	No.1	0.26	1.79	1.50	Ohno and Nishioka*	L2	0.04	1.42	0.80
	No.2	0.21	1.79	2.30	Kanda et al.*	85STC-1	0.09	1.42	1.14
	No.3	0.42	1.79	2.00		85STC-2	0.09	1.42	1.14
Ang et al.*	No.3	0.38	1.51	2.83		85STC-3	0.09	1.42	1.14
	No.4	0.21	1.51	2.22	Muguruma et al.*	AH-1	0.40	3.81	3.81
Soesianawati et al.*	No.1	0.10	1.51	0.86		BL-1	0.25	3.81	3.81
	No.2	0.30	1.51	1.22		BH-1	0.25	3.81	3.81
	No.3	0.30	1.51	0.08		BH-2	0.42	3.81	3.81
	No.4	0.30	1.51	0.06	Ono et al.*	CA060C	0.60	2.36	2.07
Zahn et al.*	No.7	0.23	1.51	1.56	Wight and Sozen*	40.048	0.15	0.61	1.44
	No.8	0.39	1.51	1.99		40.067	0.11	0.61	2.00
Watson et al.*	No.5	0.50	1.51	1.22	Atalay and Penzien*	No.1S1	0.10	1.67	1.54
	No.6	0.50	1.51	0.58		No.2S1	0.09	1.67	0.93
Tanaka and Park*	No.1	0.20	1.57	2.55		No.3S1	0.10	1.67	1.54
	No.2	0.20	1.57	2.55		No.5S1	0.20	1.67	1.54
	No.3	0.20	1.57	2.55		No.6S1	0.18	1.67	0.93
	No.4	0.20	1.57	2.55		No.9	0.26	1.67	1.54
	No.5	0.10	1.25	1.70		No.10	0.27	1.67	0.93
	No.6	0.10	1.25	1.70		No.11	0.28	1.67	1.54
	No.7	0.30	1.25	2.08		No.12	0.27	1.67	0.93
	No.8	0.30	1.25	2.08	Azizinami et al.*	NC-2	0.21	1.95	2.19
Park and Priestley*	No.9	0.10	1.88	2.17		NC-4	0.31	1.95	1.26
					Nagasaka*	HPRC19-32	0.34	1.33	1.66
Shear failure group									
Imai and Yamamoto*	No.1	0.07	2.09	0.73	Li et al. [13]	1DH	0.29	3.10	3.23
Arakawa et al.*	OA2	0.19	3.13	0.53		1NL	0.1	3.10	0.59
	OA5	0.45	3.13	0.53		1NH	0.29	3.10	0.59
Umehara and Jirsa*	CUW	0.17	3.06	0.97		2DL	0.09	3.10	3.23
Lynn et al. [9]	3CLH18	0.09	3.12	0.16		2DH	0.3	3.10	3.23
	CMH18	0.26	3.12	0.16		2NL	0.1	3.10	0.59
	CMD12	0.26	3.12	0.35		2NH	0.29	3.10	0.59
Matchulat [10]	K1	0.32	2.48	0.19	Li et al. [2]	3DL	0.07	3.24	1.14
	K2	0.22	2.48	0.19		3DH	0.22	3.24	1.14
Woods [11]	WoodsK3	0.62	3.12	0.19		3NL	0.07	3.24	0.25
	WoodsK4	0.17	2.48	0.49		3NH	0.23	3.24	0.25
Henkhaus [12]	#6	0.12	2.48	0.50		4DL	0.08	3.24	1.14
	#7	0.11	2.48	0.50		4DH	0.22	3.24	1.14
	#8	0.11	2.48	0.29		4NL	0.08	3.24	0.25
Li et al. [13]	1DL	0.09	3.10	3.23		4NH	0.24	3.24	0.25

* Secimen collected from Taylor et al. [8]

3. lateral load-displacement curve used in this study

Lateral load-displacement curve and its yielding point are required to define for analytical model. Since the model callibration method is executed base on energy dissipation, the experimental envelope curve is used to be the model's backbone curve. The yielding point is determined by the point reached the defined yielding strength on the envelope curve.

For flexure failure columns, the defined yielding strength is the shear strength at the yielding moment, which is calculated in Eq. (4). Both yielding moment and nominal moment are computed by Xtract.

$$V_{my} \leq 0.8V_{mn} \tag{4}$$

where V_{my} is the shear strength at the yielding moment; V_{mn} is the shear strength at the nominal moment.

For shear failure columns, the defined yielding strength is set as shear cracking strength. The formula is

$$V_{cr} \leq 0.6V_n \tag{5}$$

where V_{cr} is the shear cracking strength; V_n is the nominal shear strength.

Since the crack behavior of columns is similar to that of walls, the formulae in ACI 318-14 [14] to compute the shear cracking strength (V_{cr}) of shear walls are used to calculate the shear cracking strength of columns.

$$V_{cr} = 0.27\sqrt{f'_c}bd + \frac{Nd}{4h} \tag{6}$$

$$V_{cr} = \left[0.05\sqrt{f'_c} + \frac{h\left(0.1\sqrt{f'_c}+\frac{0.2N}{bh}\right)}{\frac{M}{V}-\frac{h}{2}}\right]bd \tag{7}$$

where b is width of the column cross section; d is effective depth of the column cross section; h is depth of the column cross section. Shear cracking strength is the lesser of Eq. (6) and Eq. (7). If $(M/V - h/2) < 0$, Eq. (7) is not applicable, and Eq. (6) should be adopted.

However, due to the different force transfor mechenism between short columns and normal columns, the nominal shear strength is calculated with different approach. Both approaches utilize the softened strut-and-tie model (SST model) proposed by Hwang and Lee [15]. For short columns, this study follows the approach suggested by Li and Hwang [1]. The main formula is

$$V_n = C_d\cos\theta = K\zeta f'_c A_{str}\cos\theta \tag{8}$$

where C_d is compressive strength of diagonal struct; θ is the angle btween diagonal strut and horizontal axis; K is strut-and-tie index; ζ is softening coefficient after reinforced concrete cracking; A_{str} is effective area at the end of diagonal strut. Due to space constraint, relevant details please refer to the literature 1 and 16.

On the other hand, this study uses the approach proposed by Li and Hwang [2] for normal columns. The shear strength of normal columns is controlled by the concrete crush strength ($V_{n,c}$) and the tensile strength ($V_{n,t}$) induced by the insufficient internal support. The concrete crush strength is calculated by the same formula in Eq. (8). The tensile strength is suggested to use the formula given in ASCE/SEI 41-13 [17] .

$$V_{n,t} = \frac{A_v f_{yt} d}{s} + \left(\frac{0.5\sqrt{f'_c}}{M/Vd}\sqrt{1+\frac{N}{0.5\sqrt{f'_c}A_g}}\right)\times 0.8A_g \tag{9}$$

where A_v is area of transverse reinforcement; f_{yt} is yielding strength of transverse reinforcement; s is spacing of transverse reinforcement; M/Vd is largest ratio of moment to shear times effective depth under loadings for the column, but shall not be taken greater than 4 or less than 2. Due to space constraint, relevant details of iterative approach please refer to the literature 2 and 16.

4. Estimation of model parameters

A systematic and standardized parameter identification method is required to identify the model parameters for minimizing the difference between experimental responses and analytic results. The parameter identification method has been developed base on energy dissipation. Simulated annealing algorithm has been used to identify model optimized parameters for each experiment. To make the hysteretic loops of the experimental response and analytic model has same initial points to calculate corresponding energy dissipation area, only the 1st hysteretic loops with different drifts in nonlinear range are chosen to be the target loop for parameters optimization.

Since model parameters control unloading and pinching behavior independently, these parameters can be optimized respectively. The entire processes have been simplified in the flowcharts as shown in Fig. 7. The indicators, named as $\alpha_{indicator}$ and $\beta_{indicator}$ shown in Eq. (10) and Eq. (11), are the ratios between experimental and analytic local energy dissipation area for each target loop. The definitions of local energy dissipation area for each parameter are shown in Fig.8 and Fig. 9. These indicators are applied to represent the effectiveness of calibration for each loop. The indicators, called $\alpha_{indicator,wavg}$ and $\beta_{indicator,wavg}$ shown in Eq. (12) and Eq. (13), are designed to report the effectiveness of calibration for whole test. When $\alpha_{indicator,wavg}$ and $\beta_{indicator,wavg}$ are close to 1, the optimized parameters called α_{exp} and β_{exp} can be identified in this stage.

$$\alpha_{\text{indicator}_i} = A_{\text{model}_i}/A_{\text{exp}_i} \tag{10}$$

$$\beta_{\text{indicator}_i} = A_{\text{model}_i}/A_{\text{exp}_i} \tag{11}$$

$$\alpha_{\text{indicator}_{wavg}} = \frac{\sum_{j=1}^{n} P_{max1_j} \times \alpha_{indicator1} + P_{max2_j} \times \alpha_{indicator2}}{\sum_{i=1}^{n} P_{max1_j} + P_{max2_j}} \tag{12}$$

$$\beta_{\text{indicator}_{wavg}} = \frac{\sum_{j=1}^{n} P_{max1_j} \times \beta_{indicator1} + P_{max2_j} \times \beta_{indicator2}}{\sum_{i=1}^{n} P_{max1_j} + P_{max2_j}} \tag{13}$$

where i is the direction of loading, i = 1 is positive, i = 2 is negative; P_{max1_j} is maximum strength in the positive direction at jth target loop; P_{max2_j} is maximum strength in the negative direction at j-th target loop; j is number of target loop;

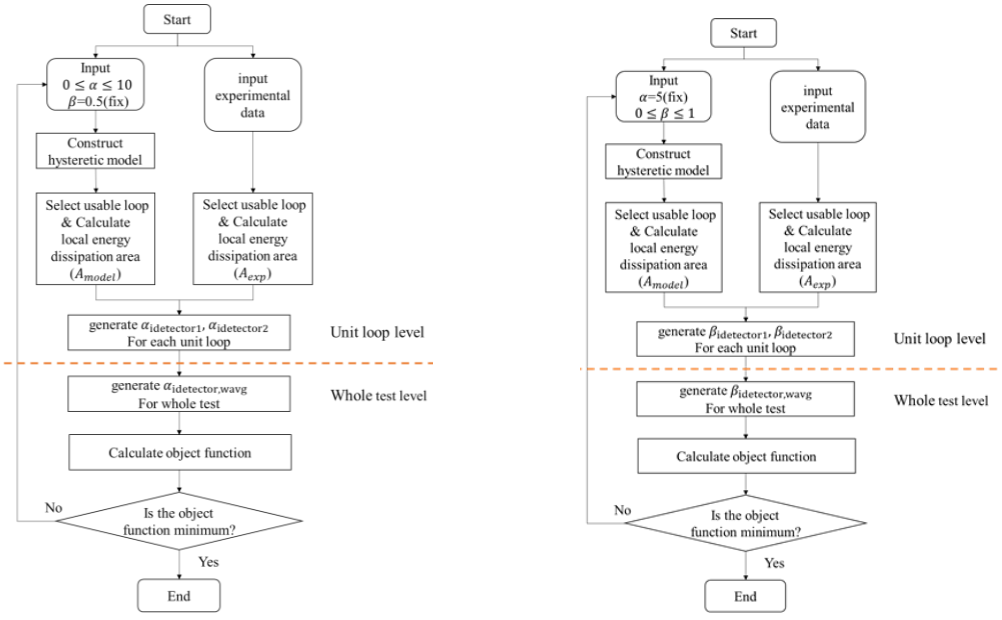

(a) α parameter (b) β parameter

Fig. 7. Flowcharts for estimation of model parameters

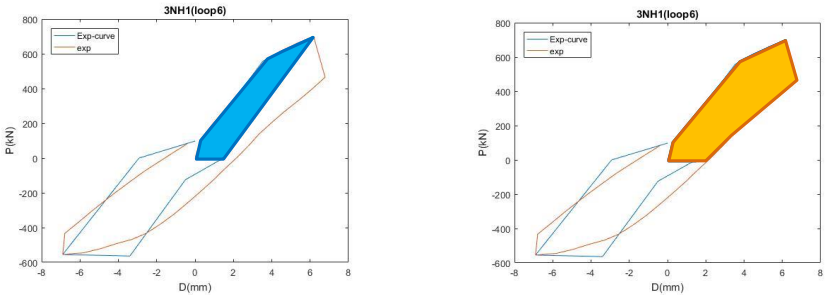

(a) analysis (b) experiment

Fig. 8. Local dissipation area for $\alpha_{\text{indicator}_1}$

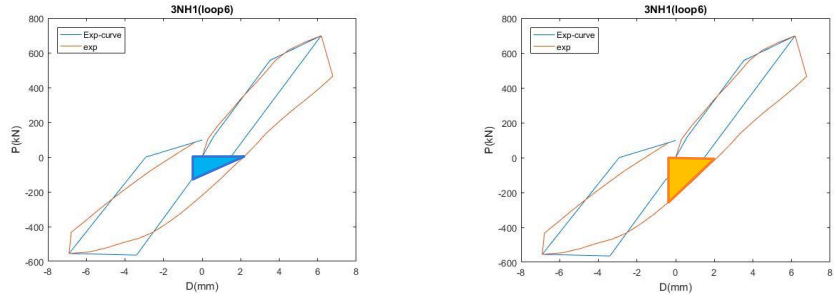

(a) analysis (b) experiment

Fig. 9. Local dissipation area for $\beta_{\text{indicator}_1}$

5. Correlation between the column physical parameters and model parameters

The linear multiplied regression analysis is used for finding the correlation between model parameters and the column physical dimensionless parameters such as axial load ratio ($N/A_g f_c'$), longitudinal reinforcement ratio (ρ_ℓ), the volumetric ratio of shear reinforcement (ρ_t), Aspect ratio (L/h). The p-value in hypothesis test as shown in Table 2 is used to select the main physical parameter. The regression equations are obtained as

For flexure failure columns,

$$\alpha_{reg} = 2.05 \times \left(\frac{N}{A_g f_c'}\right)^{-0.50} \times (\rho_\ell)^{-0.48} \times (\rho_t)^{0.17} \quad (14)$$

$$\beta_{reg} = 0.69 \times \left(\frac{N}{A_g f_c'}\right)^{0.11} \times (\rho_\ell)^{0.29} \quad (15)$$

For shear failure columns,

$$\alpha_{reg} = 0.09 \times \left(\frac{N}{A_g f_c'}\right)^{-0.52} \times (\rho_\ell)^{2.74} \times (\rho_t)^{0.35} \quad (16)$$

$$\beta_{reg} = 0.69 \times (\rho_t)^{-0.24} \times \left(\frac{L}{h}\right)^{0.25} \quad (17)$$

Table 2. The p-value in hypothesis test

	Model parameter	$\frac{N}{A_g f_c'}$	ρ_ℓ	ρ_t	$\frac{L}{h}$	R^2
Flexure failure column	α	V (0.00024)	V (0.003)	V (0.03)	---	0.53
	β	V (0.05)	V (0.007)	---	---	0.27
Shear failure column	α	V (0.0005)	V (0.0002)	V (0.0016)	---	0.64
	β	---	---	V (0.0088)	V (0.028)	0.53

6. Equation optimization base on energy dissipated area

The equations of model parameters by regression analysis is not directly related to the calibration result. Hence, the model parameters computed in Eq. (14) to Eq. (17) could not perform well on response calibration. The equation optimization method is developed by extending the aforementioned parameter identification method. The entire process has been abridged in the flowcharts as shown in Fig. 10. By optimizing the constant in Eq. (14) to Eq. (17), the object function in Eq. (18) is designed to search the equation which has minimum mean square error on the view of energy dissipated area.

$$\mathrm{MSE} = \sum_{i=1}^{n} \left(\alpha_{indicator_{wavg,i}} - 1\right)^2 \tag{18}$$

where n is the total number of the column datasets; i is the i-th column datasets.

the new equations of model parameters are obtained as:

For flexure failure columns,

$$\alpha_{\mathrm{cal}} = 0.15 \times \left(\frac{N}{A_g f_c'}\right)^{-2} \times (\rho_\ell)^{-3} \times (\rho_t) + 2.5 \leq 10 \tag{19}$$

$$\beta_{\mathrm{cal}} = 0.5 \times \left(\frac{N}{A_g f_c'}\right)^{0.65} \times (\rho_\ell)^{0.7} + 0.4 \leq 1 \tag{20}$$

For shear failure columns,

$$\alpha_{\mathrm{cal}} = 0.15 \times \left(\frac{N}{A_g f_c'}\right)^{-2} \times (\rho_\ell)^{-3} \times (\rho_t) + 2.5 \leq 10 \tag{21}$$

$$\beta_{\mathrm{cal}} = 0.5 \times \left(\frac{N}{A_g f_c'}\right)^{0.65} \times (\rho_\ell)^{0.7} + 0.4 \leq 1 \tag{22}$$

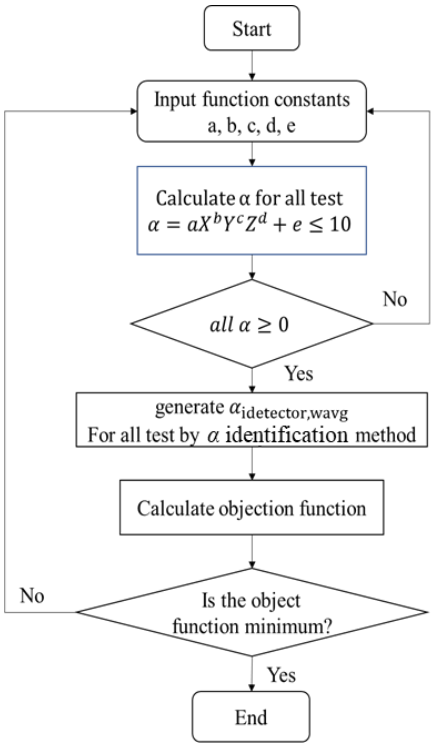

Fig. 10. Flowcharts for equation optimization

7. Parameter verification and comparison with Sharma et al. [7] proposed equation

To verify the Pivot hysteretic model parameters and to compare with the parameters computed by Sharma et al. [7] equations shown in Eq. (1) and Eq. (2), comparison between experimental and analytical load - displacement plots of all cyclic tests in literature have been graphed base on Sharma et al. equations and proposed equations shown in Eq. (19) to Eq. (22) respectively. Because of the space constraint, only the plots of tests by Ang et al. [18] have been presented for flexure failure columns in Fig. 11, and the plots of tests by Li et al. [13] have been presented for shear failure columns in Fig. 12. To compare the effectiveness on hysteretic modeling by these equations, the ratio of experimental and analytical accumulative dissipated energy at the cycle reached limit point are computed individually. The ratios for all flexure failure column specimens are plotted in Fig. 13, and the ratios for all shear failure column specimens are plotted in Fig. 14. The result shows that the analytical models based on the parameters suggested by Sharma et al. have worse performance and underestimated the dissipated energy due to ignoring the effect in different failure mode. On the other hand, it can be clearly said that parameters proposed in this paper can simulate the hysteretic behavior of columns in different failure mode well and reasonable.

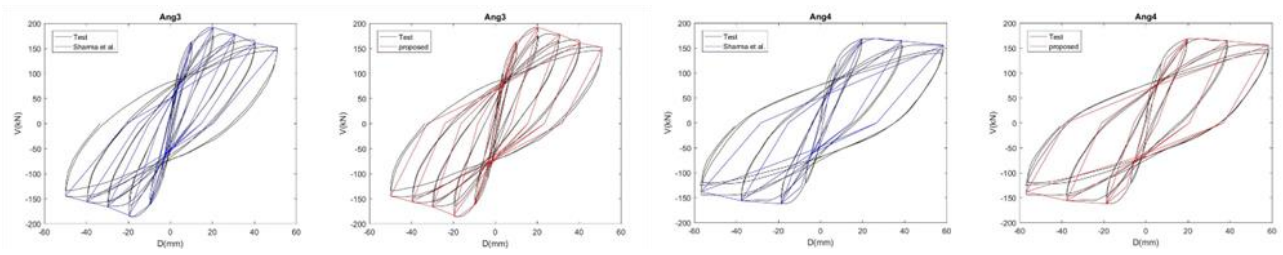

(a) No.3 (Sharma et al.) (b) No.3 (proposed) (c) No.4 (Sharma et al.) (d) No.4 (proposed)

Fig. 11. Comparison between experimental and analytical load-displacement plots of tests by Ang et al. [18]

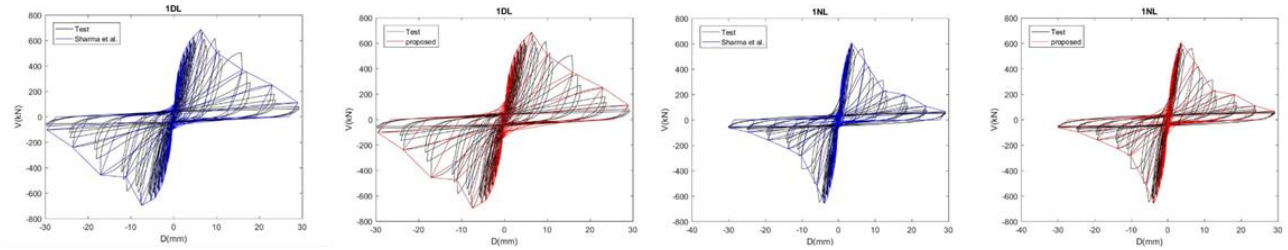

(a) 1DL (Sharma et al.) (b) 1DL (proposed) (c) 1NL (Sharma et al.) (d) 1NL (proposed)

Fig. 12. Comparison between experimental and analytical load-displacement plots of tests by Li et al. [13]

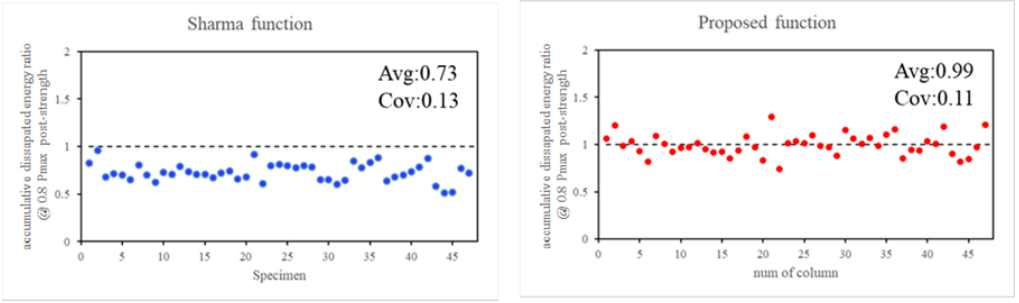

(a) Sharma et al. equations (b) proposed equations

Fig. 13. The experimental and analytical accumulative dissipated energy ratio for all tests

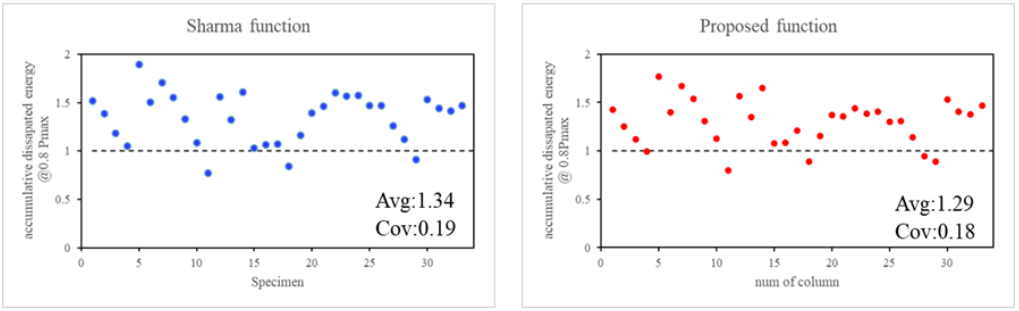

(a) Sharma et al. equations (b) proposed equations

Fig. 14. The experimental and analytical accumulative dissipated energy ratio for all tests

8. Conclusion

This paper presents the new equations of model parameters to predict the hysteretic behavior of reinforced concrete columns in different failure mode based on Pivot hysteretic model. To calibrate the proposed model with the experiment results accurately, a series of analytical methods executed base on dissipated energy has been developed by using Simulated annealing, nonlinear regression analysis and hypothesis test. By parameter verification and comparison with Sharma et al. equations, it is necessary to take the effect in different failure modes into consider for hysteretic modeling and the parameters computed by proposed equations can simulate the hysteretic behavior of columns in different failure mode well and reasonable.

9. Acknowledgement

This study was funded by the Ministry of Science and Technology (MOST) through funding MOST 108-2625-M-002-002.

10. Reference

[1] Li YA, Hwang SJ (2017): Prediction of Lateral Load Displacement Curves for Reinforced Concrete Short Columns Failed in Shear. *Journal of Structural Engineering, ASCE,* 143(2), DOI: 10.1061/(ASCE)ST.1943-541X.0001656, 04016164.

[2] Li YA, Weng PW, Hwang SJ (2019): Seismic Performance of RC Intermediate Short Columns Failed in Shear. *ACI Structural Journal,* Vol. 116, No. 3, pp. 195-206.

[3] Chiou TC, Hsiao FP, Chung LL, Weng JH, Li CH, Liu CC, Xue Q, Ho YS, Chen SJ, Yang CP, Weng PW, Shen WC, Tu YS, Yang YS, Li YA, Yeh YK, Hwang SJ (2018): Taiwan Earthquake Assessment for Structures by Pushover Analysis (TEASPA V3.1). *Technical Report NCREE-18-015,* National Center for Research on Earthquake Engineering, Taipei, Taiwan. (In Chinese)

[4] Clough RW, Johnston SB (1966): Effect of stiffness degradation on earthquake ductility requirements. *Proceedings of 2nd Japan Earthquake Engineering Symposium*, Tokyo, Japan

[5] Takeda T, Sozen MA, Nielsen NN (1970): Reinforced Concrete Response to Simulated Earthquakes. *Journal of Structural Divisions, ASCE,* Vol. 96, No.12, pp. 2557-2573.

[6] Dowell RK, Seible F, Wilson EL (1998): Pivot Hysteresis Model for Reinforced Concrete Members. *ACI Structural Journal,* Vol. 95, No. 5, pp. 607-617.

[7] Sharma A, Eligehausen R, Reddy GR (2013): Pivot Hysteresis Model Parameters for Reinforced Concrete Columns, Joints, and Structures. *ACI Structural Journal,* Vol. 110, No. 2, pp. 217-228.

[8] Taylor AW, Kuo C, Wellenius K, Chung D (1997): A Summary of Cyclic Lateral Load Tests on Rectangular Reinforced Concrete Columns. *NISTIR 5984,* Building and Fire Research Laboratory, National Institute of Standards and Technology, United States Department of Commerce, Technology Administration.

[9] Lynn A, Moehle J, Mahin S, Holmes W (1996): Seismic Evaluation of Existing Reinforced Concrete Columns. *Earthq. Spectra,* Vol. 12, No. 4, pp. 715–739.

[10] Matchulat L (2009): Mitigation of Collapse Risk in Vulnerable Concrete Buildings. *M.S. thesis,* Univ. of Kansas, Lawrence, KS.

[11] Woods C (2010): Displacement Demand Effects in Vulnerable Reinforced Concrete Columns. *M.S. thesis*, Univ. of Kansas, Lawrence, KS.

[12] Henkhaus K, Pujol S, Ramirez J (2013): Axial Failure of Reinforced Concrete Columns Damaged by Shear Reversals. *Journal of Structural Engineering, ASCE,* Vol. 139, No. 9, pp. 1172-1180.

[13] Li YA, Huang YT, Hwang SJ (2014): Seismic Response of Reinforced Concrete Short Columns Failed in Shear. A*CI Structural Journal,* Vol. 111, No. 4, pp. 945-954.

[14] ACI (2014): Building code requirements for structural concrete (ACI 318-14) and commentary (ACI 318R-14). *ACI Committee 318,* Farmington Hills, MI.

[15] Hwang SJ, Lee HJ (2002): Strength Prediction for Discontinuity Regions by Softened Strut-and-Tie Model. *Journal of Structural Engineering, ASCE,* Vol. 128, No. 12, pp. 1519-1526.

[16] Hwang SJ, Tsai RJ, Lam WK, Moehle JP (2017): Simplification of Softened Strut-and-Tie Model for Strength Prediction of Discontinuity Regions. *ACI Structural Journal,* Vol. 114, No. 5, pp. 1239-1248.

[17] ASCE (2014): Seismic evaluation and retrofit of existing buildings (41-13). *ASCE/SEI 41-13,* Reston, VA.

[18] Ang BG, Priestley MJN, Park R (1981): Ductility of Reinforced Bridge Piers Under Seismic Loading. *Report 81-3,* Department of Civil Engineering, University of Canterbury, Christchurch, New Zealand, 109 pp.

